# Surface sulfate modified $TiO_2$ visible light active photocatalyst for complex wastewater purification: preparation, characterization and photocatalytic activity

Lilla Balassa[a,*], Áron Ágoston[a,*], Zsolt Kása[b], Viktória Hornok[a] and László Janovák[a**]

[a] *Department of Physical Chemistry and Materials Sciences, University of Szeged, H-6720 Szeged, Aradi V.sqr.1, Hungary*

[b] *Department of Organic Chemistry, University of Szeged, H-6720 Szeged, Dóm sqr. 8, Hungary*

* *These authors share the first authorship*

** *Corresponding authors. Tel.: +36 62 544 210; Fax: +36 62 544 042.*
*E-mail address: janovakl@chem.u-szeged.hu (László Janovák)*

## Abstract

One of the major concerns of today's society is the rapid deterioration of our environment. Wastewater purification via catalysts could be a solution for a part of this situation. Related to this topic. Related to this topic here we report the facile preparation of surface-modified $TiO_2$ photocatalyst performed by simply grinding and calcination process, using elemental sulfur originated from the desulfurization of petroleum.

Visible light active (Eg = 2.91 eV) sulfur modified $TiO_2$ were prepared with low surface charge (-62.2 ± 0.7 mV). The improved photocatalytic activity of sulfated samples was proved via benzoic acid photodegradation tests under visible light and compared to the reference P25. According to the results, the sulfated $TiO_2$ degraded 41% of the initial benzoic acid, while TiO2 degraded only 27%. Next mechanically stable photoreactive composite layers were prepared using the ST-benzene catalyst and it was presented that the thin film can successfully degrade the model water. In the complex sample, the ST-benzene containing photocatalyst layer's efficiency was 25.3% for phenol, 20.3% for niacin, 30.0% for paracetamol, 10.6% for caffeine and 28.8% for imidacloprid respectively. In addition, it is also presented that the sulfated photocatalyst is able to generate more hydroxyl radicals (which depends on the reaction rate

constant of 7-hydroxycoumarin formation, $k_{ST\text{-}benzene} = 6.682 \times 10^{-5}$ $\mu mol \times L^{-1} \times s^{-1}$) than the initial P25 $TiO_2$, which makes it a promising photocatalyst for water purification.

**Keywords:** Sulfated $TiO_2$, Visible light activity, Water purification, Real/complex model wastewater, OH radical, Immobilization

## 1. Introduction

Environmental problems have not yet been solved due to consumer society, so the catalyst development is an intensively researched field, for both environmental and economic reasons. One of the biggest economic and social problems of our time is the state of our waters. Clean drinking water is unfortunately very limited and the increasing amount of wastewater is also harmful to the environment [1,2], so it is highly necessary to purify the waters. From the chemical treatments, the advanced oxidation processes (AOPs) is one of the most commonly used methods, *e. g.* heterogeneous photocatalysis, photolysis, catalytic ozonation [3]. Realistic testing is essential for successful cleaning technology development, therefore instead of photocatalytic degradation of just one molecule as a model pollutant, it is recommended to make a real model wastewater that contains the most common pollutants in water, *e. g.* surfactants, aromatic organic molecules, pesticides, preservative materials [4]. Effectiveness in decomposing not only one kind of molecule but being effective in a complex, multi-component system can increase the value of a photocatalyst.

Heterogeneous photocatalysis gained much attention over the past decades [5,6]. The application of various semiconductor photocatalysts in the fields of environmental protection or water purification has become very notable [7,8]. When it was irradiated with UV- or visible light, these materials show photooxidative properties. Photons having higher energy than the bandgap can excite the semiconductors, consequently, the electrons can get from the valence band to the conduction band, and an electron-hole pair arise [9]. This charge separation can promote redox reactions on the surface of the catalyst, so during these photooxidative processes, reactive oxygen species could generate, which could responsible for the decomposition of pollutants [10]. Since Fujishima and Honda reported the water splitting effect of titanium dioxide ($TiO_2$) under ultraviolet light, this photocatalyst has gained great attention among researchers [11]. $TiO_2$ is a very promising material since it has high photocatalytic activity, high stability, chemical inertness, low toxicity and low cost[12,13]. Regarding applications as a photocatalyst the main drawback of the $TiO_2$ is its bandgap, namely the rutile phase has ~3,02

eV, while the anatase has ~3,2 eV, respectively, which means that it can be excited only with UV light ($\lambda$<~390 nm) irradiation [14]. Since the UV region of solar light is only about 5% [15], there have been various attempts to modify the catalyst to extend its absorption wavelength into the visible light region. There are two favored ways for modification: doping is when the crystalline structure was modified and decoration when the surface of $TiO_2$ was modified.

Doping $TiO_2$ with various elements (e.g. N, S, C, Fe, Cu) can reduce the bandgap energy, therefore it could be activated with UV and visible light as well [16–18]. On the other hand, the dopant can act as an electron trap, which slows down the recombination of the electron-hole pairs so that also favors the photocatalytic activity. It has been proven that modifying $TiO_2$ with sulfur *via* different methods can help enhance the photocatalytic efficiency under visible light [19,20]. In our previous work, we presented a simple method to synthesize a visible light active sulfated $TiO_2$ from dissolved elemental sulfur. Carrying on with this path, in this work we use different solvents to prepare S-$TiO_2$.

In the case of heterogeneous photocatalysis, the decomposition of pollutants is due to the production of reactive oxygen species such as hydroxyl radical, $H_2O_2$, superoxide anion, hydroperoxide radical, peroxide radicals, hydroxyl anion [5]. Due to its high oxidation potential (2.8 V [21]), the hydroxyl radical (OH•) is one of the most oxidizing agents among them [22], thus is able to degrade the different model contaminants through several reaction pathways, such as phenol and paracetamol used in this article [23,24]. The amount of hydroxyl radical produced is critical to the efficiency of a photocatalyst, thus detection of this radical is essential. 7-hydroxycoumain formation from coumarin is due to the reaction between coumarin and hydroxyl radical, therefore the hydroxyl radical can be detectable by this method [25]. We can follow the production of the hydroxyl radical by following the amount of 7-hydroxycoumarin *via* the spectrofluorometric method.

In this work, seven different surfaces sulfated $TiO_2$ visible light active photocatalysts were prepared suitable for complex wastewater purification. Structure characterization methods were applied to prove the success of the photocatalyst preparation while diffuse-reflectance measurements were proved that the modified photocatalyst show photocatalytic activity in the visible region. Next, we determined the photocatalytic activity for all the prepared photocatalysts under visible light illumination following the degradation of the benzoic acid test molecule. Using the photocatalyst with the highest activity, photocatalytically active

composite films were also prepared to facilitate the application of the photocatalysts for water purification. The results of photocatalytic experiments show that the pollutant components of complex wastewater can be decomposed separately but even under the simultaneous presence of components as well. From the results, it can be also concluded that the highest oxidation potential hydroxyl radical shows a competitive process during the photodegradation.

## 2. Materials and methods

### 2.1. Catalyst preparation

Sulfur-modified titanium dioxide ($TiO_2$) samples were prepared using sulfur solutions with different media and solvents. Propanol (99.8%, MOLAR), 2-propanol (≥99.8%, Sigma-Aldrich), dimethylformamide (reagent grade, Merck), butanol (99.9%, MOLAR), toluene (99.99%, MOLAR), xylene (>99%, Merck) and also benzene (for comparison) (99.93%, Lachner) were tested, the consequent samples names are indicated in **Table 1.** 1-propanol, 2-propanol and butanol were chosen to study how the sulfation works with aliphatic solvents, dimethylformamide for how sulfation works with a heteroatom-containing solvent, both toluene and xylene are aromatic like benzene, but less toxic, so we chose these solvents to find a less toxic medium instead of benzene. First, the sulfur powder (≥99.5%, Sigma-Aldrich) was dissolved in 10 mL solvents, to achieve 60.2 mg/L sulfur concentration. Next 2 mL as-prepared sulfur-solutions were added to 1-1 g of commercially available $TiO_2$ (Degussa P25) powder to achieve 3 at.% sulfur content and the obtained mixture was then ground and dried at 120 °C for 4 hours (the grinding was repeated every hour through the drying process). The samples were then calcinated for 3 hours at 200 °C in airflow to oxidize the surface precipitated sulfur to sulfate.

### 2.2. Photocatalytic thin film preparation

The photocatalyst thin films were prepared by spray-coating technique with gravity feed airbrush (ChroMax BD-203) gun with 3 bar operation pressure on the 5×5 cm glass plates [26], to obtain 1 mg/cm$^2$ surface coverage. The S-$TiO_2$ nanoparticles were also immobilized in polyacrylate binder [poly(ethyl-acrylate co methyl-methacrylate)] (obtained from Evonik Industries, Germany) matrix. In this case, the photocatalyst/polymer mass ratio was 8/2. During the preparation of this coating material nitrogen gas flow was used to avoid undesirable reactions.

### 2.3. Modell wastewater preparation

We prepared a complex wastewater sample for modeling real wastewater for the photocatalytic experiment. The model wastewater contained several chemical compounds, all of which represent a group of compounds present in an undesired concentration in average communal wastewater. Niacin (vitamin B3) modeling the antioxidant, paracetamol as drug, imidacloprid as pesticide (insecticide), phenol modeling the high aromatic pollutant and caffeine because its quantity increases in the environment and it could be harmful to the environment [27]. Although niacin is not harmful, but real wastewater contains niacin and it also affects the photocatalytic processes [28]. The initial concentration of the test molecules was 10 mg/L in all cases.

### 2.4. Characterization

The sulfur-modified $TiO_2$ samples crystallinity were determined with X-ray diffraction measurements, which were carried out with a Philips X-ray diffractometer (PW 1830 generator, PW 1820 goniometer, $CuK_\alpha$: $\lambda$= 0.1542 nm, 40-50 kV, 30-40 mA), from 10 to 60° (2Θ), at room temperature.

The Fourier transform infrared (FT-IR) spectra were recorded with an Avatar 330 FT-IR Thermo Nicolet spectrophotometer with a middle IR source and optics. The samples were pastilled with KBr before measurement. The spectra measured between 4000 and 500 $cm^{-1}$, while the applied resolution was 1 $cm^{-1}$.

For optical characterization, the diffuse reflectance spectra were recorded with Ocean Optics UV-VIS USB4000 type, diode array spectrophotometer. The spectrums were recorded from 200 to 850 nm wavelength. The bandgap values were determined using the Kubelka-Munk method [29].

The electrophoretic mobility of samples was measured with a HORIBA SZ-100 Nanoparticle Analyzer. The measurements were performed with a disposable carbon-coated electrode cell. The zeta-potential values were determined using the Smoluchowski model. For the measurements, dispersions were prepared in 0.001 w/v% concentration from the sulfur modified $TiO_2$ samples, as well as from the commercially available P25 $TiO_2$ for comparison.

The hydrodynamic stability of photocatalysts in the aqueous phase can be also studied with the zeta-potential values.

The morphologies of the samples were analyzed by a JEOL JEM-1400plus (JEOL Ltd., Tokyo, Japan) transmission electron microscope (TEM) operating with 120 kV accelerating voltage on Formal foil covered 200 mesh copper grids.

### 2.5. Mechanical stability of photocatalytic thin films

The presence of binding polymer in the composite photoreactive thin films increases the stability against physical effects. The mechanical stability of the 100% photocatalyst layer and the prepared S-$TiO_2$/polymer (8/2) thin film was tested by crocking tests, with TABER Crockmeter 418. On the fixed sample plate (5×5 cm) an acrylic cylinder made alternating motion. One back and forth movement was one cycle and the weight loss was measured as a function of the number of crocking abrasive cycles. The chosen photocatalyst was the ST-benzene for this abrasive test.

### 2.6. Photocatalytic activity measurements

The photocatalytic efficiency of the ST-X samples was measured in aqueous suspension at room temperature. In the first case, the model pollutant was benzoic acid and the experiments were performed in an opened glass reactor. The used light source was fixed at 5 cm distance from the surface of continuously agitated (4000 rpm) 50 mL suspensions. The light source used during the photocatalytic tests mainly emits in the visible light range (local $\lambda_{max}$= 610 nm, 544 nm, 489 nm, 435 nm and 405 nm) and it also contains a small amount of UV light (local $\lambda_{max}$= 366 nm and 314 nm) (**Fig. 1A.**) The photocatalyst concentration of suspension was 0.005 wt%, while the benzoic acid initial concentration was 20 mg/L, the irradiation time was 120 min. The decreasing concentration of the model pollutant was followed by a Thermo Scientific DIONEX ICS-6000 high-performance ion chromatograph which was equipped with a conductivity detector, the column was a DIONEX IonPac AS11-HC-4μm, the eluent was 30 mmol/L KOH, which was generated by an eluent generator and the conductivity of the eluent was neutralized before the detector. Before the irradiation, the suspension was kept in the dark for 30 min to ensure the adsorption equilibrium. The collected samples were centrifuged two times and filtered through 0.1 μm Millex-VV PVDF filter before ion chromatographic analysis.

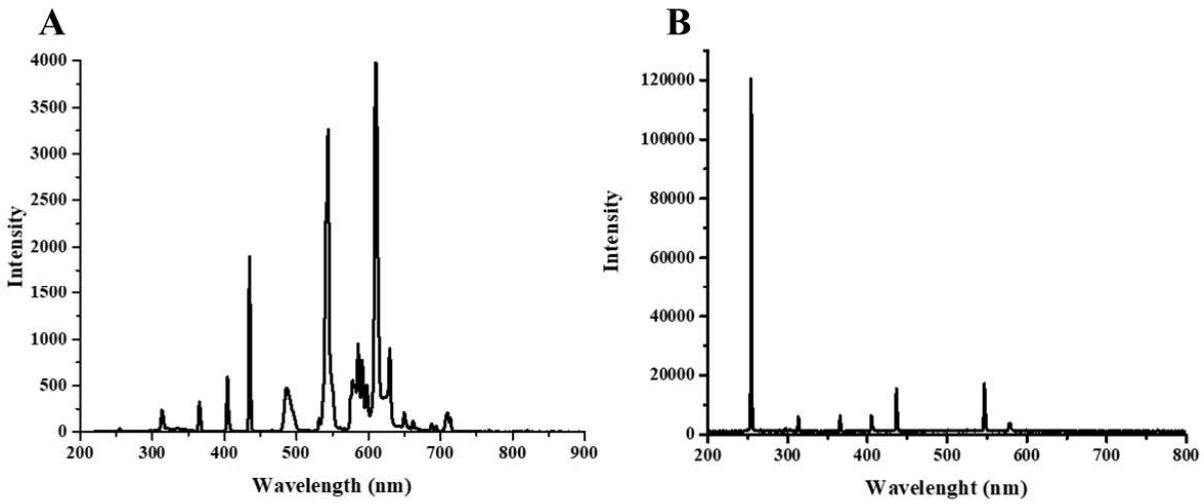


**Figure 1.** The emission spectra of used Visible light source (LightTech visible light CELL lamp) (A) and the emission spectra of used UV light source for surface activation (LightTech GCL307T5L/CELL) (B)

In the second case, the prepared complex wastewater degradation measured on the photocatalytic composite thin films (photocatalyst/polymer ratio was 8/2). Before the measurements the composite surface was activated with high-intensity UV light (LightTech GCL307T5L/CELL) for 180 minutes from a distance of 5 cm. As reported earlier, this process ensures the partial photodegradation of the polymer component in the composite layer, consequently, the concentration of the photocatalyst particles is increasing on the surface region [26]. The spectrum of the light source used for surface activation can be seen in **Fig. 1B.** , it contains mainly UV photons with $\lambda_{max}$= 254 nm and only a small amount of visible light (local $\lambda_{max}$= 436 nm and 547 nm). The as-prepared photocatalytic thin film (5×5 cm) was placed in the center of 50 mL solution, the used light source was the same (**Fig. 1A.**) and it was fixed from the surface of solution at 5 cm distance, the irradiation time was 300 min. The concentrations of the components in the model wastewater were followed by an Agilent 1290 Infinity II liquid chromatography with UV detector attached to an Agilent 6470 ESI-MS/MS detector. The stationary phase was an InfinityLab Poroshell 120 EC-C18, while the mobile phase was 20/80 methanol/water with 1 mL/min flow rate. Furthermore, the eluent contained 0.1% formic acid due to increase the ionization potential of the pollutant [30]. The six-point calibrations were performed for the following target ions in positive MS mode: Niacin: 124.1, Paracetamol: 152.2, Caffeine: 195.2, Imidacloprid: 256.7. Furthermore, in the case of each compound 3 qualifier ion was used. The phenol concentration was monitored only by the UV

detector at 210 nm. Before the irradiation, the suspension was also kept in dark for 30 min to ensure the adsorption equilibrium. After these previous measurements, the photocatalytic experiments were run separately for each component of the complex wastewater, to determine their disturbing effect under simultaneous presence. In this this way it may be revealed which component decomposes more by hydroxyl radical and which through hole-side oxidation.

### 2.7. Detection of hydroxyl radical

The hydroxyl radicals are detectable by their reaction with coumarin. If hydroxide is present in the system, 7-OH-coumarin will form from coumarin [25]. Before the measurements the composite surface with 20 wt.% polymer content was activated by UV light (LightTech GCL307T5L/CELL) for 180 minutes from a distance of 5 cm. Hydroxyl radical production capacity was measured on both the initial $TiO_2$ and ST-X containing samples with the highest photocatalytic activity.

The experiments were preceded by the calibration of spectrofluorometer with 7-hydroxycoumarin and the concentration dependence was linear over the range used ($1\times10^{-8}$ mol/L – $5\times10^{-6}$ mol/L), the equation of calibration curve was $I = 4.789\times10^{8} \times c_{7\text{-hydroxycoumarin}} + 1.306$, $R^2 = 0.9999$. During the visible light illuminated (**Fig. 1A.**) measurements the initial concentration of coumarin was $1\times10^{-4}$ mol/L. The photocatalytic layer was placed in the center of the solution, the surface of the solution was at 5 cm distance from the light source. The 7-hydroxycoumarin concentration change was determined by a Jasco FP-8500 spectrofluorometer. The excitation wavelength of 7-hydroxycoumarin was 345 nm while the detection wavelength was 453 nm. Before the measurements, the samples were centrifuged two times to completely remove the dispersed photocatalyst particles.

## 3. Results and discussion

### 3.1. Characterization

After the synthesis, the crystal phase of the photocatalyst obtained was determined by XRD measurements. The characteristic reflection peaks of the initial and modified samples were at the same 2Θ angle values and the ratio of the peaks is also similar indicating that neither the lattice nor the crystal phase changed after the surface sulfation processes (**Fig 2.**). The (110), (101*), (211*) peaks belong to the rutile phase and the (101), (103), (004), (200) (211) peaks belong to the anatase phase [31]. XRD pattern for $TiO_2$ (Degussa P25) was assigned by the help

of anatase JCPDS card (No 21-1272) and rutile JCPDS card (No 21-1276). The crystallite size, which was determined by the Scherrer equation was not changed significantly since the values varied between 20.24 and 23.61 nm (**Table 1.**). These values were calculated from the full-width at the half-maximum intensity of the (101) diffraction peak.

From the FT-IR measurements, we can determine not only the presence of possible changes, but also the new specific bonds, so this method can prove the success of the preparation. **Fig. 3.** shows the FT-IR spectra of $TiO_2$ and the photocatalyticly most active (see later) sulfated $TiO_2$ sample (ST-benzene) in the range of 2000-1000 $cm^{-1}$, ST-benzene was the only sulfated $TiO_2$ where the characteristic vibrations of sulfate were detectable at this low (3 at.%) sulfur content. In the spectra, a strong vibrational signal was detected at 1631 $cm^{-1}$ which was contributed to the bending vibration of the O–H group, (this typically appears between 1660 $cm^{-1}$ and 1600 $cm^{-1}$), due to the adsorbed $H_2O$ [32]. The intensity of this peak is higher with sulfate content [33].

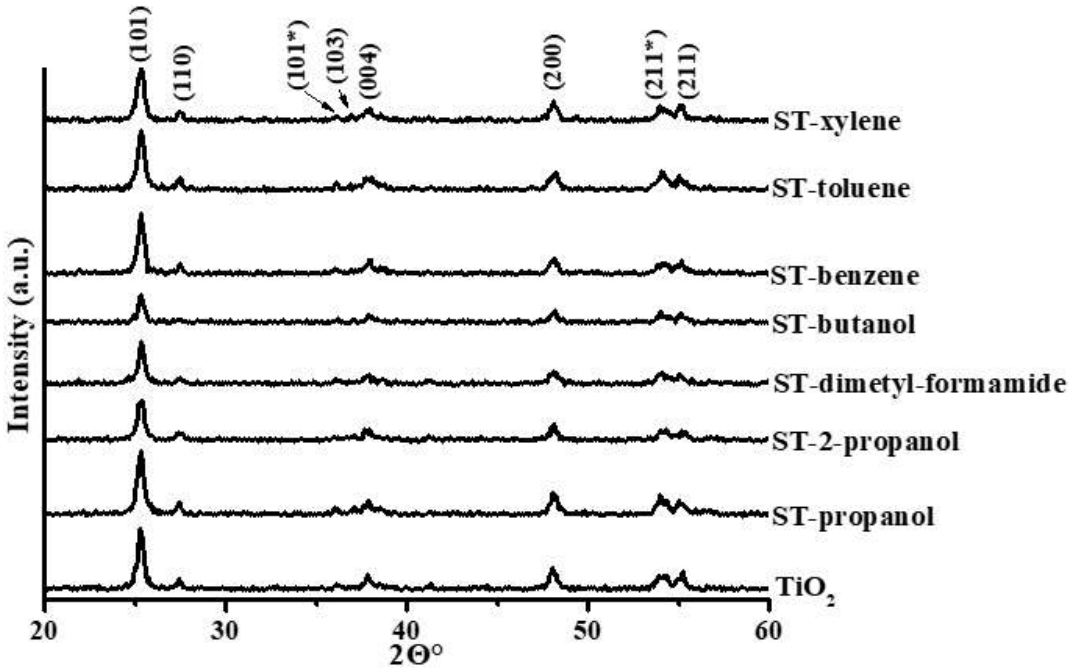


**Figure 2.** XRD patterns of $TiO_2$ and ST-X samples

**1. Table.** The bandgap ($E_g$), excitation wavelength and crystal size values of the ST-X samples

| Sample name | $E_g$ (eV) * | Excitation wavelength** (nm) | Crystal size*** (nm) |
|---|---|---|---|
| $TiO_2$ | 3.17 | 391 | 22.27 |
| ST-1-propanol | 2.89 | 429 | 20.24 |
| ST-2-propanol | 2.88 | 430 | 21.25 |
| ST-dimethylformamide | 2.97 | 417 | 22.37 |
| ST-butanol | 2.98 | 416 | 23.61 |
| ST-benzene | 2.92 | 425 | 23.61 |
| ST-toluene | 3.00 | 413 | 22.37 |
| ST-xylene | 3.00 | 412 | 22.37 |

* Determined by Kubelka-Munk equation [29]

** Calculated by Planck–Einstein relation from measured bandgap value (photon energy) [34]

*** Determined by Scherrer-equation [35]

Between 1220 $cm^{-1}$ and 1170 $cm^{-1}$, the symmetric stretching vibration frequency of the S=O bond appeared [36], while the signal at 1130 $cm^{-1}$ was contributed to the S–O vibration. Specifically, this frequency belongs to the bidentate $SO_4^{2-}$ group, which binds to $Ti^{4+}$ ion [33]. Furthermore, the vibration at 1040 $cm^{-1}$ is the asymmetric stretching valance vibration of the S=O bond [37]. From 400 $cm^{-1}$ to 800 $cm^{-1}$ is the Ti–O–Ti and Ti–O stretching vibration [38]. Thus, based on the detected vibrations, it can be concluded that sulfation was especially successful for one of the samples (ST-benzene). Since the modification only occurred on the photocatalyst surface, XRD measurements were inappropriate to identify these surface structural changes.

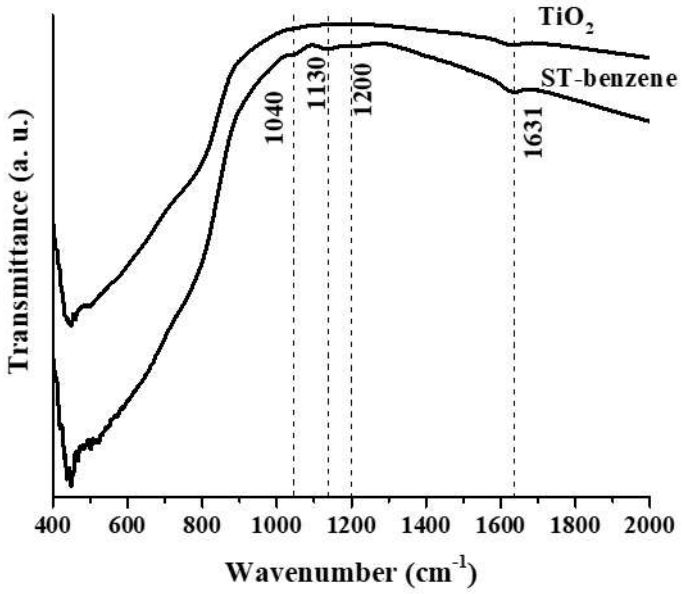


**Figure 3.** FTIR spectra of $TiO_2$ and ST-benzene samples

According to the diffuse reflectance measurements (**Fig. 4.**) with our simple sulfation method we can decrease the bandgap energy, the absorption edges of modified catalysts were shifted to the visible light range, so the prepared photocatalysts can be excited by visible light. After the measurements, the corresponding band gaps were calculated using the Kubelka-Munk equation from DR spectra [29]. **Fig. 4B.** shows the determination of the bandgap of the $TiO_2$ and ST-X samples from DR spectra by the Kubelka-Munk method. All the ST-X samples with slight yellowish color (see inserted photos) show light absorption in the visible region. The calculated $E_g$ values are shown in **Table 1.** and they are varied between 2.88 eV and 3.00 eV ($TiO_2$ was 3.17 eV), which means that these photocatalysts could be excited by visible light, with $\lambda$=430.5 nm or lower wavelengths. The ST-benzene sample has a local photon absorption maximum at 460 nm (2.7 eV).

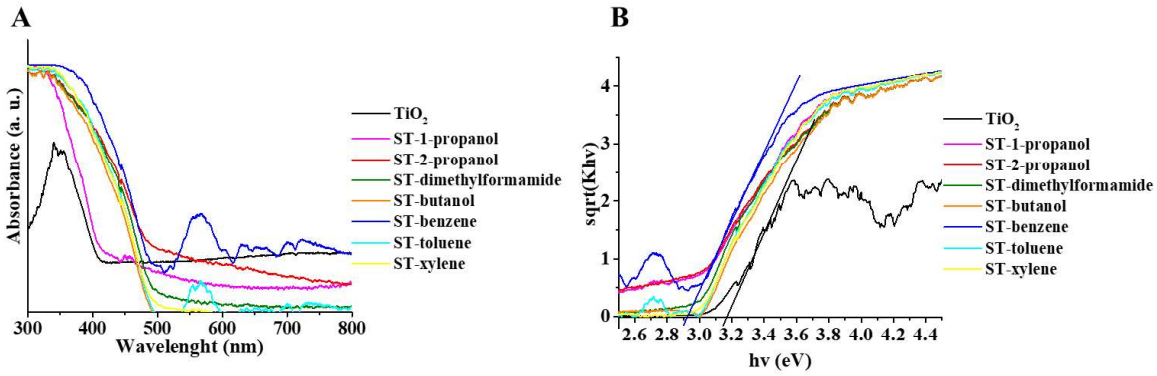


**Figure 4.** The absorption spectra of $TiO_2$ and ST-X samples (A) and Kubleka-Munk representation of $TiO_2$ and ST-X samples for bandgap energy determination (B)

The zeta potential of the ST-X samples prepared in different solvents is illustrated in **Fig. 5.** The initial P25 $TiO_2$ was also measured for reference and its zeta potential was -26.3 ± 2.1 mV at pH around 8.10. Compared to the initial P25 $TiO_2$ the sulfated samples have a lower surface charge, ranging from -28.4 mV to -62.2 mV and they had also lower pH, around 5.4 in distilled water. Among the sulfated $TiO_2$ samples the ST-benzene has the lowest zeta potential (-62.2 ± 0.7 mV) probably because most of the surface sulfur on the $TiO_2$ was converted to sulfate so benzene was the most effective solvent from the series. The results indicate that the modification of the initial P25 $TiO_2$ with sulfur lowered the surface charge of the samples, *i.e.* the sulfate group present on the surface of $TiO_2$ nanoparticles results decrease in the zeta potential, this is also confirmed by sulfation.

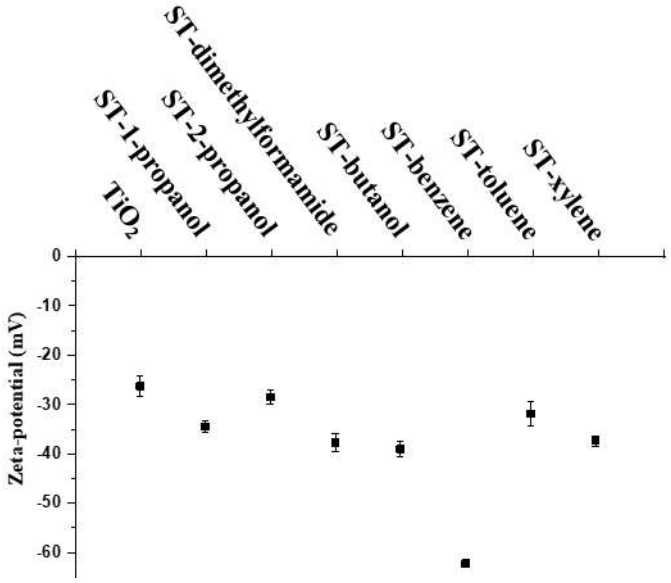


**Figure 5.** The zeta-potential values of 0.001 wt.% aqueous dispersion of the initial $TiO_2$ (pH=8.10) and ST-X samples (pH=5.4)

The images in **Fig. 6** also confirmed that the sulfur modification process did not result in sulfur nanoparticles or other elemental sulfur deposits on the surface of the $TiO_2$. It can also be stated that no aggregation occurred during the treatment, which could reduce the specific surface area.

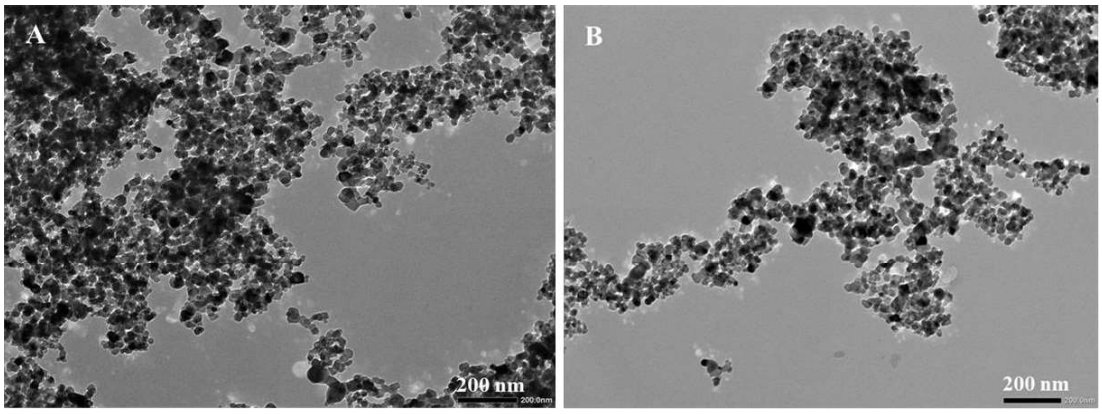


**Figure 6.** TEM images of the sample $TiO_2$ (A) and the sample ST-benzene

### 3.2. Mechanical stability of photocatalytic thin films

For the practical application, the initial stability of the photocatalyst was improved by a polymeric binder material to get photoreactive thin films with enhanced wear-resistant properties. Furthermore, the presence of polymer could also prevent the soaking of the photocatalyst particles during the application in an aqueous environment. As the results in **Fig. 7** indicate, the two layers had different mechanical stability, from the layer which contains

100% photocatalyst the semiconductor particles were totally worn-out even after one abrasion cycle. However, in the case of the composite layer with 20% polymer content, even after 15 abrasion cycles, ~20% of the initial film remains on the surface, so the presence of binding polymer increased the mechanical stability resulted a well-used self-cleaning photocatalytic surface.

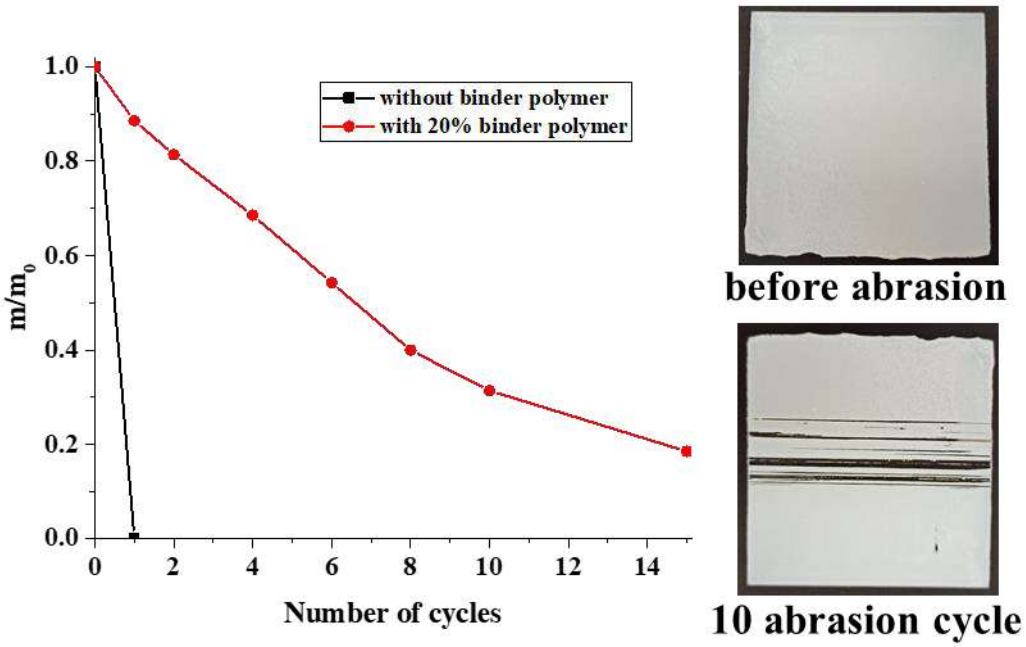


**Figure 7.** Weight loss as a function of abrasion cycles, on the film of ST-benzene without and with polymer after the crocking

### 3.3. Photocatalytic activity measurements

Firstly, we calibrated the ion chromatograph with benzoic acid, and the concentration dependence was linear over the range used (1-50 mg/L). The photocatalytic experiments were performed for the initial $TiO_2$ and each sulfated photocatalyst (**Fig. 8.)**

The results show that the ST-benzene has the highest photocatalytic activity from the synthesized photocatalysts for benzoic acid decomposition, higher than the pure $TiO_2$, which degrade only 27% of the initial benzoic acid while ST-benzene degraded 41%. It may suggest, that the surface decorated sulfate groups could increase the photocatalytic activity. ST-benzene is more effective than the other ST-X samples, probably because benzene is the most apolar

solvent from the series. Both toluene and xylene are aromatic but less apolar than benzene, which could be detrimental to atomic dissolution.

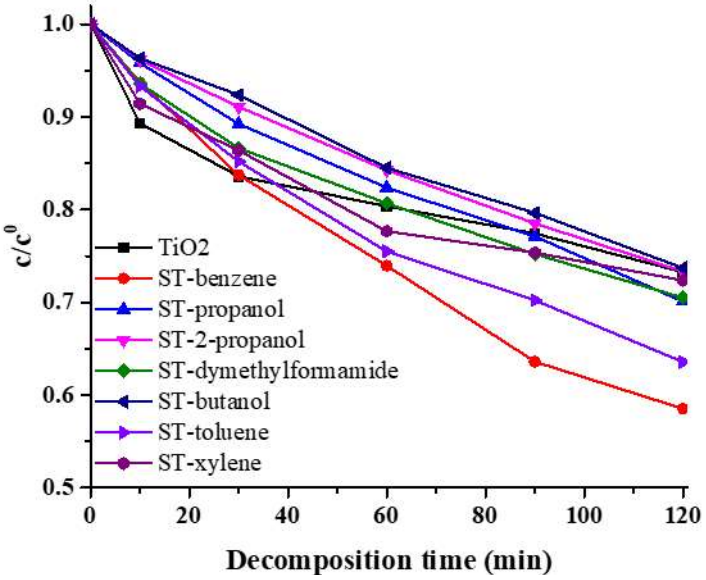


**Figure 8.** Photocatalytic activity of the ST-X photocatalysts and reference $TiO_2$ in aqueous suspension, under visible light illumination

In the case of the model wastewater, the photocatalytic experiment was performed only with the most active ST-benzene photocatalyst compared to reference P25 $TiO_2$. The LC-MS/MS conditions allow the separation of the components and the possible intermediated products in the sample during the measurements. From the results in **Fig. 9.** we can demonstrate that the synthesized photocatalyst can relatively efficiently decompose all the used pollutants even in the simultaneous presence of them under visible light activation (separate photocatalytic experiments (ss) and complex sample (cs)). In the case of experiments with complex wastewater phenol was degraded by 34.7%, niacin by 32.2%, paracetamol by 40%, caffeine by 20.5% and imidacloprid by 78.5% from the initial amount after 6 h irradiation. **Fig. 10** shows the same photooxidation curves in the case of $TiO_2$ reference photocatalyst. For comparisons, phenol was degraded by 25.3%, niacin by 20.3%, paracetamol by 30.0%, caffeine by 10.6% and imidacloprid by 28.8% from the initial amount. These results indicate that the photocatalytic activity of initial $TiO_2$ was weaker for all components compared to the sulfated $TiO_2$.

Next, the photodegradation of contaminant components was also examined separately. According to the single-component degradation test carried out with ST-benzene sulfated

photocatalyst, the pollutants degraded to a greater extent (phenol by 65%, niacin by 33.2%, paracetamol by 91.5%, caffeine by 80.1% and imidacloprid by 88.9%), than in the multicomponent model wastewater. This finding is also true for the reference $TiO_2$ since phenol was degraded by 47.3%, niacin by 29.9%, paracetamol 75.3%, caffeine 55.4% and imidacloprid by 86.3%),. This was to be expected, but it also appears that the catalyst was able to degrade all components even in complex samples. As regarding the real concentration of the pollutants that occur in wastewaters, it can be said that our model phenol concentration was significantly lower [39] compared to wastewater one while the other components occur in higher concentration [40-41]). Consequently, the as-prepared sulfated photocatalyst has a relatively high degradation capacity. The above results show how photocatalytically induced reactions are affected by an efficient radical scavenger, which here is the niacin. The main radical is the hydroxyl radical [42], wherewith niacin reacts faster than with other components [28]. Since the degradation rates of phenol, paracetamol and caffeine were lower in the complex sample, therefore these components were degraded mainly by hydroxyl radical which is also confirmed in the literature [23,24,43]. Caffeine reacts with hydroxyl radical only through one reaction pathway [43] while phenol and paracetamol can react with hydroxyl radical through various pathways due to their aromatic structure [23,24]. This can be a possible explanation for the decreased degradation in the multicomponent system -compared to the separate experiment (see a comparison of dashed and continuous lines in **Fig. 9.** and **Fig. 10.**). The degradation of imidacloprid barely changed –compared to the separate experiment- in the case of ST-benzene (from 80.1% to 78.5%) but in the case of $TiO_2$, there was a significant change (from 86.3% to 47.6%). Imidacloprid degraded considerably on another reaction way, in this case, surface decomposition occurs with direct oxidation on the surface by hole side oxidation and reaction with hydroxyl radical adsorbed on the surface [44]. Since niacin concentration is much smaller (not detectable) in true wastewater as we used in the present work, it cannot remove consume the hydroxyl radical as a scavenger and therefore the degradation of the other components could be much more efficient.

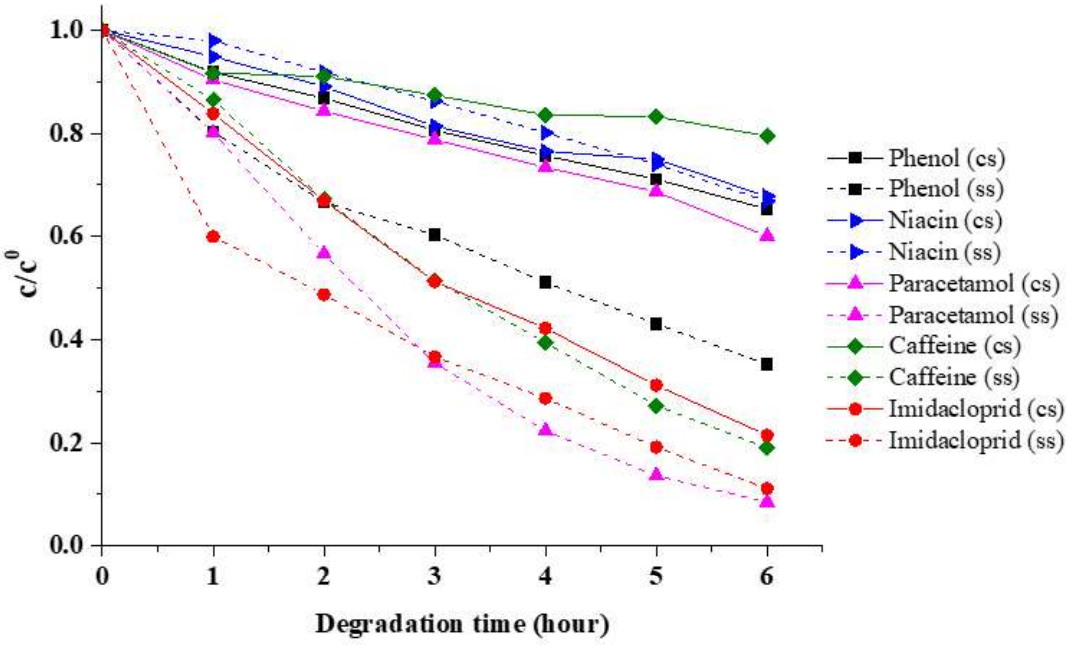


**Figure 9.** Photocatalytic activity of ST-benzene photocatalyst on photocatalytic thin film under visible light irradiation (cs- in a complex sample, ss- in separated sample)

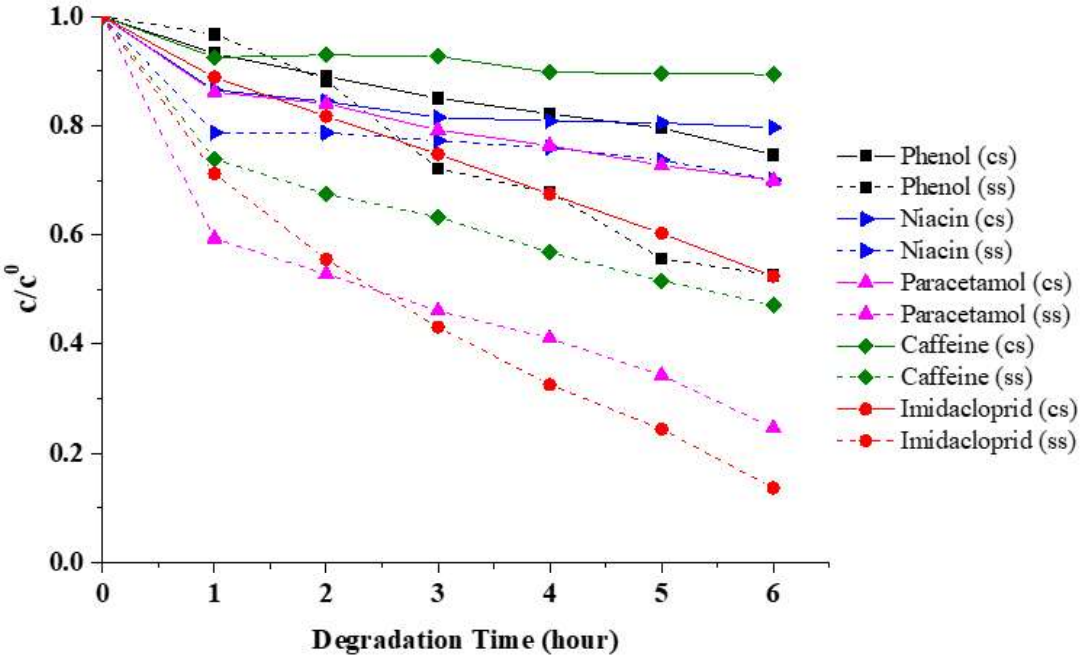


**Figure 10.** Photocatalytic activity of $TiO_2$ photocatalyst on photocatalytic thin film under visible light irradiation (cs- in a complex sample, ss- in separated sample)

### 3.4. Detection of hydroxyl radical

Without a catalyst, 7-hydroxyoumarin was not detected, as only the hydroxyl radicals formed during the photocatalytic process can produce 7-hydroxycoumarin. From the results we can see that the ST-benzene has higher hydroxyl radical production capacity, because the sulfate on the surface has electron trapping ability [33], so the charge separation takes longer, therefore, more water molecules could be oxidized on the hole side. In **Fig. 11.** shown the 7-hydroxycoumarins formation kinetic was slower in the case of $TiO_2$ than on ST-benzene modified $TiO_2$ since the corresponding rate constants ($k_{7\text{-hydroxycoumarin}}$) were $5.607\times10^{-5}$ and $6.682\times10^{-5}$ $\mu mol\times L^{-1}\times s^{-1}$, respectively.

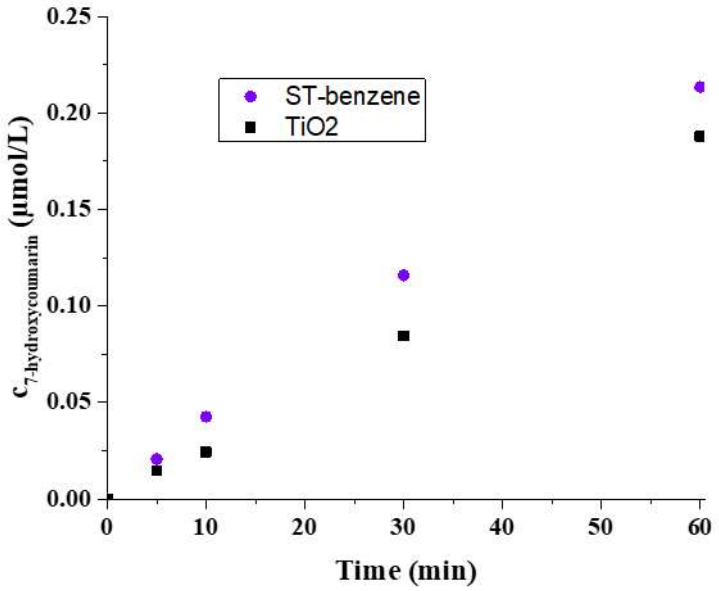


**Figure 11.** Production kinetic of 7-hydroxycoumarin from coumarin on the surface of $TiO_2$ and ST-benzene contain photocatalytic thin film (A=25 $cm^2$, 1 $mg/cm^2$ specific surface area)

### Conclusion

Sulfur modified $TiO_2$ photocatalyst was synthesized with improved ROS producing ability and visible light activity. The results show that photocatalyst sulfation is best achieved with sulfur dissolved in benzene (0.164 $g_{benzoic\ acid}/1g_{cat}$ decomposed by ST-benzene), as the solubility is almost the same as in other solvents (e.g. toluene), so the success is probably due to the nonpolar nature of benzene, a property that is very different for solvents. The obtained sulfated $TiO_2$ samples have lower band gap energies (2.88-3.00 eV) than $TiO_2$ (3.17 eV), this

means that the sample can be excited by visible light. Moreover, according to the electrokinetic measurements, the surface sulfation was also affected the surface charge since the initial zeta potential of $TiO_2$ (-26.3 ± 2.1) was decreased in all cases (from -28.4 ± 1.5 mV to -62.2 ± 0.7 mV) and the lowest value (-62.2 ± 0.7 mV) was achieved in the case of ST-benzene $TiO_2$ photocatalysts. The higher zeta potential values of sulfated $TiO_2$ ensure sufficient repulsive force to attain better colloidal stability and consequently, the system can be more easily kept in a homogeneous suspension, therefore the particles are more easily accessible to the photons, explaining the improved photocatalytic activity. Next, the sulfated $TiO_2$ with optimized sulfur content was incorporated into polyacrylate-based binder material in order to prepare a visible-light active photoreactive composite layer with improved mechanical stability. It can be stated that the prepared photocatalyst not only works in a monomolecular system, but it is also able to degrade the components side by side even in a complex, multi-component system. In the case of the multi-component photocatalytic experiments, the results show that the phenol, niacin, paracetamol and caffeine degraded mainly with hydroxyl radical while the imidacloprid degraded with surface decomposition. Since the hydroxyl radical can decompose the most pollutants the fastest the concentration of OH· was also determined as a function of irradiation time. These results proved that the reason for the increase in photocatalytic activity is obviously due to the generation of more hydroxyl radicals (which depends on the reaction rate constant of 7-hydroxycoumarin formation, $k_{ST\text{-}benzene} = 6.682\times10^{-5}$ $\mu mol\times L^{-1}\times s^{-1}$), caused by the more efficient oxidation of water. This is due to the longer charge separation, all of which is good evidence of the ability of the sulfate on the surface to electron trap. So, the surface modification of the initial $TiO_2$ occurred by simply grinding and calcination using elemental sulfur from the desulfurization of petroleum.

## Acknowledgments

The authors are very thankful for the financial support from the National Research, Development and Innovation Office (GINOP-2.3.2-15-2016-00013 and GINOP-1.1.2-PIACI-KFI-2021-00193). This paper was also supported by the UNKP-20-5 New National Excellence Program of the Ministry for Innovation and Technology from the source of the National Research, Development and Innovation Fund and by the János Bolyai Research Scholarship of the Hungarian Academy of Sciences.

## Author statement

Lilla Balassa: Methodology, Investigation, original draft

Áron Ágoston: Methodology, Investigation, original draft

Zsolt Kása: Methodology, Investigation, Writing - review & editing

Viktória Hornok: Investigation

László Janovák: Conceptualization, Supervision, Funding acquisition, Writing - review & editing

## Declaration of Competing Interest

The authors declare that they have no known competing financial interests or personal relationships that could have appeared to influence the work reported in this paper.

## References

[1] G. Jungclaus, V. Avila, R. Hites, Organic compounds in an industrial Wastewater: a case study of their environmental impact, Environ. Sci. Technol. 12 (2002) 88–96. https://doi.org/10.1021/ES60137A015.

[2] M. Köck-Schulmeyer, M. Villagrasa, M. López de Alda, R. Céspedes-Sánchez, F. Ventura, D. Barceló, Occurrence and behavior of pesticides in wastewater treatment plants and their environmental impact, Sci. Total Environ. 458–460 (2013) 466–476. https://doi.org/10.1016/J.SCITOTENV.2013.04.010.

[3] M.J. Farré, M.I. Franch, S. Malato, J.A. Ayllón, J. Peral, X. Doménech, Degradation of some biorecalcitrant pesticides by homogeneous and heterogeneous photocatalytic ozonation, Chemosphere. 58 (2005) 1127–1133. https://doi.org/10.1016/J.CHEMOSPHERE.2004.09.064.

[4] J. Margot, L. Rossi, D.A. Barry, C. Holliger, A review of the fate of micropollutants in wastewater treatment plants, Wiley Interdiscip. Rev. Water. 2 (2015) 457–487.

https://doi.org/10.1002/WAT2.1090.

[5] A.O. Ibhadon, P. Fitzpatrick, Heterogeneous Photocatalysis: Recent Advances and Applications, Catal. 2013, Vol. 3, Pages 189-218. 3 (2013) 189–218. https://doi.org/10.3390/CATAL3010189.

[6] A.J. Bard, Photoelectrochemistry and heterogeneous photo-catalysis at semiconductors, J. Photochem. 10 (1979) 59–75. https://doi.org/10.1016/0047-2670(79)80037-4.

[7] K. Wetchakun, N. Wetchakun, S. Sakulsermsuk, An overview of solar/visible light-driven heterogeneous photocatalysis for water purification: $TiO_2$- and ZnO-based photocatalysts used in suspension photoreactors, J. Ind. Eng. Chem. 71 (2019) 19–49. https://doi.org/10.1016/J.JIEC.2018.11.025.

[8] S.N. Ahmed, W. Haider, Heterogeneous photocatalysis and its potential applications in water and wastewater treatment: A review, Nanotechnology. (2018) Article 342001. https://doi.org/10.1088/1361-6528/aac6ea.

[9] L.-H. Reydellet, P. Roche, D.C. Glattli, B. Etienne, Y. Jin, Quantum Partition Noise of Photon-Created Electron-Hole Pairs, Phys. Rev. Lett. 90 (2003) Article 176803. https://doi.org/10.1103/PhysRevLett.90.176803.

[10] Y. Vieira, J. Leichtweis, E.L. Foletto, S. Silvestri, Reactive oxygen species-induced heterogeneous photocatalytic degradation of organic pollutant Rhodamine B by copper and zinc aluminate spinels, J. Chem. Technol. Biotechnol. 95 (2020) 791–797. https://doi.org/10.1002/JCTB.6267.

[11] A. FUJISHIMA, K. HONDA, Electrochemical Photolysis of Water at a Semiconductor Electrode, Nat. 1972 2385358. 238 (1972) 37–38. https://doi.org/10.1038/238037a0.

[12] P.L. Sanches, L.R.D.O. Geaquinto, R. Cruz, D.C. Schuck, M. Lorencini, J.M. Granjeiro, A.R.L. Ribeiro, Toxicity evaluation of $TiO_2$ nanoparticles on the 3d skin model: A systematic review, Front. Bioeng. Biotechnol. (2020) Article 575. https://doi.org/10.3389/fbioe.2020.00575.

[13] E. Nascimben Santos, Á. Ágoston, S. Kertész, C. Hodúr, Z. László, Z. Pap, Z. Kása, T. Alapi, S.A.G. Krishnan, G. Arthanareeswaran, K. Hernadi, G. Veréb, Investigation of the applicability of $TiO_2$, $BiVO_4$, and $WO_3$ nanomaterials for advanced photocatalytic

membranes used for oil-in-water emulsion separation, Asia-Pacific J. Chem. Eng. 15 (2020) Article 2549. https://doi.org/10.1002/apj.2549.

[14] C. Han, M. Pelaez, V. Likodimos, A.G. Kontos, P. Falaras, K. O'Shea, D.D. Dionysiou, Innovative visible light-activated sulfur doped $TiO_2$ films for water treatment, Appl. Catal. B Environ. (2011) 77-87. https://doi.org/10.1016/j.apcatb.2011.06.039.

[15] X. Hu, Y. Li, J. Tian, H. Yang, H. Cui, Highly efficient full solar spectrum (UV-vis-NIR) photocatalytic performance of $Ag_2S$ quantum dot/$TiO_2$ nanobelt heterostructures, J. Ind. Eng. Chem. (2017) 189-196. https://doi.org/10.1016/j.jiec.2016.09.022.

[16] T. Boningari, S.N.R. Inturi, M. Suidan, P.G. Smirniotis, Novel one-step synthesis of nitrogen-doped $TiO_2$ by flame aerosol technique for visible-light photocatalysis: Effect of synthesis parameters and secondary nitrogen (N) source, Chem. Eng. J. (2018) 324-334. https://doi.org/10.1016/j.cej.2018.05.122.

[17] L. Galeano, S. Valencia, G. Restrepo, J.M. Marín, Dry-co-grinding of doped $TiO_2$ with nitrogen, silicon or selenium for enhanced photocatalytic activity under UV/visible and visible light irradiation for environmental applications, Mater. Sci. Semicond. Process. (2019) 47-57. https://doi.org/10.1016/j.mssp.2018.10.032.

[18] V. Kumaravel, S. Mathew, J. Bartlett, S.C. Pillai, Photocatalytic hydrogen production using metal doped $TiO_2$: A review of recent advances, Appl. Catal. B Environ. (2019) 1021-1064. https://doi.org/10.1016/j.apcatb.2018.11.080.

[19] Z. He, J. Tang, J. Shen, J. Chen, S. Song, Enhancement of photocatalytic reduction of $CO_2$ to $CH_4$ over $TiO_2$ nanosheets by modifying with sulfuric acid, Appl. Surf. Sci. (2016) 416-427. https://doi.org/10.1016/j.apsusc.2015.12.163.

[20] S. Cravanzola, F. Cesano, F. Gaziano, D. Scarano, Sulfur-doped $TiO_2$: Structure and surface properties, Catalysts. (2017) 7070215. https://doi.org/10.3390/catal7070214.

[21] G. Palmisano, M. Addamo, V. Augugliaro, T. Caronna, A. Di Paola, E.G. López, V. Loddo, G. Marcì, L. Palmisano, M. Schiavello, Selectivity of hydroxyl radical in the partial oxidation of aromatic compounds in heterogeneous photocatalysis, Catal. Today. 122 (2007) 118–127. https://doi.org/10.1016/J.CATTOD.2007.01.026.

[22] S. Guerra-Rodríguez, E. Rodríguez, D.N. Singh, J. Rodríguez-Chueca, Assessment of

Sulfate Radical-Based Advanced Oxidation Processes for Water and Wastewater Treatment: A Review, Water 2018, Vol. 10, Page 1828. 10 (2018) Article 1828. https://doi.org/10.3390/W10121828.

[23] P.B. Jayathilaka, G.C. Pathiraja, A. Bandara, N.D. Subasinghe, N. Nanayakkara, Theoretical study of phenol and hydroxyl radical reaction mechanism in aqueous medium by the DFT/B3LYP/6-31+G(d,p)/CPCM model, Can. J. Chem. 92 (2014) 809–813. https://doi.org/10.1139/CJC-2014-0191/ASSET/IMAGES/LARGE/CJC-2014-0191CON.JPEG.

[24] R.S. Borges, J.L.M. Do Nascimento, N. Alves, A Theoretical Study for Oxidative Metabolism of Acetaminophen, J. Comput. Theor. Nanosci. 7 (2010) 1–5. https://doi.org/10.1166/jctn.2010.1569.

[25] A.C. Maier, E.H. Iglebaek, M. Jonsson, Confirming the Formation of Hydroxyl Radicals in the Catalytic Decomposition of $H_2O_2$ on Metal Oxides Using Coumarin as a Probe, ChemCatChem. 11 (2019) 5435–5438. https://doi.org/10.1002/CCTC.201901316.

[26] L. Janovák, Á. Deák, S.P. Tallósy, D. Sebők, E. Csapó, K. Bohinc, A. Abram, I. Pálinkó, I. Dékány, Hydroxyapatite-enhanced structural, photocatalytic and antibacterial properties of photoreactive $TiO_2$/HAp/polyacrylate hybrid thin films, Surf. Coatings Technol. (2017) 316-326. https://doi.org/10.1016/j.surfcoat.2017.07.072.

[27] G.R. Quadra, J.R. Paranaíba, J. Vilas-Boas, F. Roland, A.M. Amado, N. Barros, R.J.P. Dias, S.J. Cardoso, A global trend of caffeine consumption over time and related-environmental impacts, Environ. Pollut. 256 (2020) Article 113343. https://doi.org/10.1016/J.ENVPOL.2019.113343.

[28] S. Ogata, M. Takeuchi, S. Teradaira, N. Yamamoto, K. Iwata, K. Okumura, H. Taguchi, Radical Scavenging Activities of Niacin-Related Compounds, Biosci. Biotechnol. Biochem. 66 (2002) 641–645. https://doi.org/10.1271/BBB.66.641.

[29] J.B. Gillespie, J.D. Lindberg, L.S. Laude, Kubelka-Munk Optical Coefficients for a Barium Sulfate White Reflectance Standard, Appl. Opt. (1975) 807-809. https://doi.org/10.1364/ao.14.000807.

[30] Y.H. Wang, G. Mondal, M. Butawan, R.J. Bloomer, C.R. Yates, Development of a liquid chromatography-tandem mass spectrometry (LC–MS/MS) method for characterizing

caffeine, methylliberine, and theacrine pharmacokinetics in humans, J. Chromatogr. B. 1155 (2020) Article 122278. https://doi.org/10.1016/J.JCHROMB.2020.122278.

[31] J.O. Carneiro, G. Vasconcelos, S. Azevedo, C. Jesus, C. Palha, N. Gomes, V. Teixeira, The evaluation of the thermal behaviour of a mortar based brick masonry wall coated with $TiO_2$ nanoparticles: An experimental assessment towards energy efficient buildings, Energy Build. (2014) 1-8. https://doi.org/10.1016/j.enbuild.2014.06.006.

[32] Dinya Zoltán: Infravörös spektroszkópia (Tankönyvkiadó Vállalat, 1981) - antikvarium.hu, (n.d.). https://www.antikvarium.hu/konyv/dinya-zoltan-infravoros-spektroszkopia-104723 158 (accessed November 2, 2021).

[33] L.G. Devi, R. Kavitha, Enhanced photocatalytic activity of sulfur doped $TiO_2$ for the decomposition of phenol: A new insight into the bulk and surface modification, Mater. Chem. Phys. (2014) 1300-1308. https://doi.org/10.1016/j.matchemphys.2013.11.038.

[34] F. Logiurato, Relativistic Derivations of de Broglie and Planck-Einstein Equations, (2014) J. Mod. Phys.1-7. DOI:10.4236/jmp.2014.51001.

[35] U. Holzwarth, N. Gibson, The Scherrer equation versus the "Debye-Scherrer equation," Nat. Nanotechnol. 6 (2011) 534. https://doi.org/10.1038/NNANO.2011.145.

[36] E.E. Platero, M.P. Mentruit, IR characterization of sulfated zirconia derived from zirconium sulfate, Catal. Lett. 1995 301. 30 (1994) 31–39. https://doi.org/10.1007/BF00813670.

[37] IR Spectrum Table, (n.d.). https://www.sigmaaldrich.com/HU/hu/technical-documents/technical-article/analytical-chemistry/photometry-and-reflectometry/ir-spectrum-table (accessed June 30, 2021).

[38] J.Y. Tai, K.H. Leong, P. Saravanan, A.A. Aziz, L.C. Sim, Dopant-free oxygen-rich titanium dioxide: LED light-induced photocatalysis and mechanism insight, J. Mater. Sci. 52 (2017) 11630–11642. https://doi.org/10.1007/S10853-017-1334-9/FIGURES/9.

[39] M.J. González-Muñoz, S. Luque, J.R. Álvarez, J. Coca, Recovery of phenol from aqueous solutions using hollow fibre contactors, J. Memb. Sci. 213 (2003) 181–193. https://doi.org/10.1016/S0376-7388(02)00526-4.

[40] F. Selimoğlu, E. Öbek, F. Karataş, E.I. Arslan, Ş.Y. Tatar, Determination of amounts of

some vitamin B groups in domestic wastewater treatment plants, Turkish J. Sci. Technol. 10 (2015) 1–5.

[41] S. Wu, L. Zhang, J. Chen, Paracetamol in the environment and its degradation by microorganisms, Appl. Microbiol. Biotechnol. 96 (2012) 875–884. https://doi.org/10.1007/S00253-012-4414-4/TABLES/3.

[42] V. Augugliaro, M. Bellardita, V. Loddo, G. Palmisano, L. Palmisano, S. Yurdakal, Overview on oxidation mechanisms of organic compounds by $TiO_2$ in heterogeneous photocatalysis, J. Photochem. Photobiol. C Photochem. Rev. 13 (2012) 224–245. https://doi.org/10.1016/J.JPHOTOCHEMREV.2012.04.003.

[43] J.P. Telo, A.J.S.C. Vieira, Mechanism of free radical oxidation of caffeine in aqueous solution, J. Chem. Soc. Perkin Trans. 2. 2 (1997) 1755–1758. https://doi.org/10.1039/A700944E.

[44] G. Rózsa, M. Náfrádi, T. Alapi, K. Schrantz, L. Szabó, L. Wojnárovits, E. Takács, A. Tungler, Photocatalytic, photolytic and radiolytic elimination of imidacloprid from aqueous solution: Reaction mechanism, efficiency and economic considerations, Appl. Catal. B Environ. 250 (2019) 429–439. https://doi.org/10.1016/J.APCATB.2019.01.065.

## Highlights

- Visible light active sulfated $TiO_2$ was synthetized by simple heat treatment method
- The hydroxyl radical production was increased due to the electron trapping
- Mechanically stable photocatalytically active composite layer was prepared
- Benzoic acid, phenol, caffeine, paracetamol, niacin and imidacloprid degradation
- Competition of the reaction of niacin with hydroxyl radical was presented

**CRediT authorship contribution statement**

**Lilla Balassa:** Methodology, Investigation, original draft

**Áron Ágoston:** Methodology, Investigation, original draft

**Zsolt Kása:** Methodology, Investigation, Writing - review & editing

**Viktória Hornok:** Investigation

**László Janovák:** Conceptualization, Supervision, Funding acquisition, Writing - review & editing